# Isotactic polystyrene/poly(vinyl methyl ether) blends: miscibility, crystallization and phase structure

**L. Amelino, E. Martuscelli*, C. Sellitti and C. Silvestre**
*Istituto di Ricerche su Tecnologia dei Polimeri e Reologia, CNR, Via Toiano 6, 80072 Arco Felice (Napoli), Italy*
*(Received 30 May 1989; accepted 11 October 1989)*

The dependence of the miscibility, melting behaviour, kinetics of crystallization and morphology in isotactic polystyrene/poly(vinyl methyl ether) (iPS/PVME) blends on temperature, thermal history and blend composition has been studied by using differential scanning calorimetry, scanning electron and optical microscopy and small-angle X-ray diffraction. For the blends obtained by casting, three glass transitions were detected, indicating that in the amorphous material three different phases were present: plain PVME, plain iPS and a homogeneous iPS/PVME mixture. This last phase seems to undergo phase separation by melting the sample at 270°C for 15 min. There is no detectable change in the melting behaviour of iPS in the blends with composition, indicating that the percentage of PVME in the iPS-rich phase is very small. The spherulite crystallization growth rate at a given temperature increases with increasing PVME content in the blend, whereas the overall crystallization rate is independent of composition. These results can be explained by considering the increase of the mobility of the crystallizable chains in the melt and the decrease of the nucleation rate due to the presence of PVME in the melt. It was found that during crystallization the iPS spherulites occluded droplet particles of PVME-rich phase in their intraspherulitic regions.

**(Keywords: isotactic polystyrene; poly(vinyl methyl ether); miscibility; crystallization; structure)**

## INTRODUCTION

Preliminary data concerning the influence of poly(vinyl methyl ether) (PVME) on the spherulite radial growth rate $G$ of isotactic polystyrene (iPS) were reported in a previous paper[1]. It was found that, at a given crystallization temperature $T_c$, $G$ increased as the overall PVME content in the blend increased. This effect, observed for all the range of $T_c$ investigated (130–205°C)

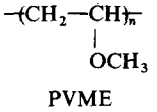

PVME

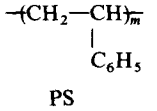

PS

and for three iPS/PVME blend composition (90/10, 80/20 and 70/30), was accounted for mainly by the fact that the $T_g$ of the crystallizable component (iPS) is larger than that of the non-crystallizable one. Then this polymer, acting partially as a diluent, produces a decrease of the melt viscosity and hence of the energy for transport of macromolecules in the melt, $\Delta F^*$. Such an effect probably predominates over the increase in the energy required to form a nucleous of critical size, $\Delta\phi^*$, and the enhancement of the spherulite growth rate results.

PVME and atactic polystyrene (aPS) have been shown to be compatible at room temperature under certain preparation conditions[2,3]. The blend presents lower critical solution temperature (*LCST*) behaviour, with a miscibility region dependent on the molecular weight of the components[4–8]. Infra-red spectroscopy has been used to determine the chemical nature of the PS/PVME interaction[6,7]. It was found that the electrons of the ether group interact with the aromatic ring of polystyrene. The interaction parameter has been measured by vapour sorption and SANS experiments. All studies confirm that $\chi_{1,2}$ is negative and approaches zero with increasing PVME content in the blend.

The results of a comprehensive investigation concerning the study of the influence of blend composition and crystallization conditions on the overall process of crystallization, on the thermal behaviour and on the phase structure are reported in the present paper in the case of iPS/PVME system. In addition, through this study we aimed to obtain information on the influence of tacticity of polystyrene on the miscibility with PVME.

## EXPERIMENTAL

### *Material and blend preparation*

The molecular characteristics of the polymers used in the present work are reported in *Table 1*. The blends were prepared by casting from toluene at about 60°C.

### *Calorimetric measurements*

The overall kinetics of crystallization and the thermal properties of the homopolymers and blends were analysed by d.s.c. (Mettler TA 3000).

* To whom correspondence should be addressed

0032-3861/90/061051-07

**Table 1** Number- and weight-average molecular weights $\bar{M}_n$ and $\bar{M}_w$, melting temperature $T'_m$ and degree of crystallinity $X_c$ as determined by differential scanning calorimetry of isotactic polystyrene and poly(methyl vinyl ether) used in the present paper

| Sample | $\bar{M}_n$ | $\bar{M}_w$ | $\bar{M}_w/\bar{M}_n$ | $T_g$ (K) | $T'_m$ (K) | $X_c$ |
|---|---|---|---|---|---|---|
| iPS | 134000 | 971000 | 7.2 | 370 | 493 | 0.29 |
| PMVE | 34000 | 65000 | 1.9 | 246 | – | – |

The isothermal crystallization process was studied using the following procedure. The samples were heated up to 270°C and kept at this temperature for 15 min under nitrogen. The samples were then rapidly cooled to the desired crystallization temperature $T_c$ and allowed to crystallize for different intervals of time. The samples were then melted and the crystallinity developed by the material was measured from the melting peak as a function of the permanence time at $T_c$. The weight fraction of the material crystallized at time $t$ was calculated from the ratio of the crystallinity developed by the material kept at $T_c$ for an interval of time $t$ to the maximum crystallinity of the material, corresponding to the completion of crystallization (overnight crystallization at $T_c$).

The observed calorimetric melting temperatures $T'_m$ and the apparent enthalpies of melting $\Delta H^*$ of the isothermally crystallized samples were obtained from the maxima and the area of the melting peaks, respectively. The samples were heated directly from $T_c$ to the melting point at a scanning rate of 5 K $min^{-1}$.

The glass transition temperatures of the materials were obtained by heating the samples (about 10 mg) from −190 to 270°C at the rate of 10 K $min^{-1}$ and by recording the heat evolved during the scanning process as a function of temperature. The $T_g$ of the sample was taken as the temperature corresponding to 50% of the transition.

*Optical microscopy*

Isothermal crystallization and measurements of the radial growth rate $G$ of iPS spherulites were performed by using an optical polarizing microscope fitted with an automatic hot stage.

The following procedure was utilized. Blend films were sandwiched between a microscope slide and a coverglass, heated at 40°C above the melting point of iPS (270°C) and kept for 15 min at this temperature. Then the temperature was rapidly lowered to the pre-fixed crystallization temperature $T_c$ and the sample allowed to crystallize. The radial growth of an iPS spherulite was monitored during crystallization, taking photomicrographs at appropriate intervals of time $t$. From the slopes of the straight lines obtained by plotting the radius against the time, $G$ was derived for all the range of $T_c$ investigated (130–200°C).

*Small-angle X-ray scattering and scanning electron microscopy*

SAXS patterns (Cu Kα, Ni-filtered radiation) were collected by a Rigaku Denki photographic camera using a collimation pinhole system and a sample–film distance of 300 mm. From such patterns the long spacing $L$ was derived by applying the Bragg law.

A morphological analysis by means of SEM scanning electron microscopy (501 Philips) was carried out on cryogenic fracture surfaces of films of iPS and blends as obtained by casting and isothermally crystallized.

## RESULTS AND DISCUSSION

*Glass transition and miscibility*

*Figure 1* reports the d.s.c. thermograms relative to the starting plain homopolymers and the blends as obtained by casting. All the blends show three glass transitions. The $T_g$ values as a function of composition are reported in *Table 2*. The presence of these three $T_g$ values could indicate that, in the amorphous system, three different amorphous phases are present: the highest $T_g$ could be relative to plain iPS, the lowest $T_g$ to plain PVME and the intermediate $T_g$ to a homogeneous iPS/PVME mixture. Therefore, the intermediate $T_g$, which is composition-dependent, could indicate that only part of our system is miscible. The presence of this miscibile phase could be due to the broad molecular-weight

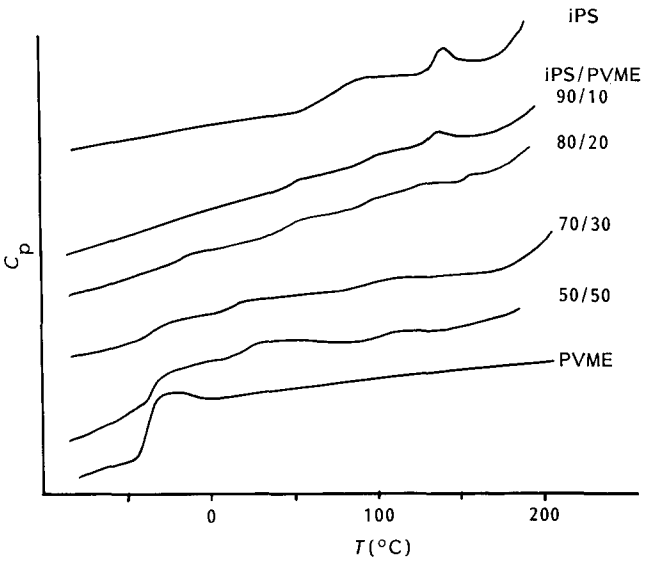


**Figure 1** D.s.c. traces of films of iPS and iPS/PVME blends obtained by casting

**Table 2** Glass transition temperatures as a function of blend composition

(a) First d.s.c. run

| Composition, iPS/PVME | $T_g$ (°C) | | |
|---|---|---|---|
| 100/0 | 97 | – | – |
| 90/10 | 100 | 52 | undetectable |
| 80/20 | 100 | 59 | undetectable |
| 70/30 | 103 | 25 | −23 |
| 50/50 | 106 | 29 | −25 |
| 0/100 | – | – | −27 |

(b) second d.s.c. run

| Composition, iPS/PVME | $T_g$ (°C) | |
|---|---|---|
| 100/0 | 97 | – |
| 90/10 | 92 | −20 |
| 80/20 | 92 | −22 |
| 70/30 | 91 | −21 |
| 50/50 | 93 | −23 |
| 0/100 | – | −27 |

distribution of the blend components, especially iPS. The molecules with lower molecular weight could form a homogeneous mixture, whereas the higher-molecular-weight chains of the components remain phase-separated.

This hypothesis seems to be confirmed by the fact that the $T_g$ values relative to iPS in the blends seem to increase with the increase of PVME content (see *Table 2*). Following our hypothesis the increase of $T_g$ could be a consequence of the increase of the concentration in the iPS phase of molecules of higher molecular weight.

It is interesting to compare the $T_g$ of this system with those reported in the literature for the system atactic polystyrene/poly(vinyl methyl ether)[8], with almost the same molecular weight of the components. For this latter blend a single $T_g$, composition-dependent, is always detected below $T=150°C$. Such a result indicates that aPS and PVME are completely miscible at temperatures where iPS and PVME are found to be only partially miscible and/or phase-separated.

This finding suggests that PS with regular molecular configuration in the amorphous phase is less miscible with PVME than is the aPS. Similar conclusions were reached in other studies on the influence of the tacticity of polystyrene and poly(methyl methacrylate) on the miscibility of polystyrene/poly(*o*-chlorostyrene-*co*-*p*-chlorostyrene) (PS/P(*o*CS-*co*-*p*CS))[9] and poly(ethylene oxide)/poly(methyl methacrylate) (PEO/PMMA)[10] systems. In particular, it was found that the iPS/P(*o*CS-*co*-*p*CS) and the PEO/iPMMA blends were less miscible than the aPS/P(*o*CS-*co*-*p*CS) and PEO/a PMMA blends, respectively.

The values of $T_g$ of the iPS/PVME films were measured also after the samples were melted at 270°C for 15 min and rapidly quenched at low temperature, in order to state the phase situation in the melt from which the isothermal crystallization, after cooling, takes place. The thermograms obtained are reported in *Figure 2*. It is possible to observe that two glass transitions are present for the blends. These $T_g$ values are slightly different from those of the homopolymers but almost constant with composition. These two $T_g$ values could indicate that in the melt two phases are present: one rich in iPS and the other rich in PVME. In particular, it could be noted that the $T_g$ of the iPS-rich phase (92°C) is lower than that of

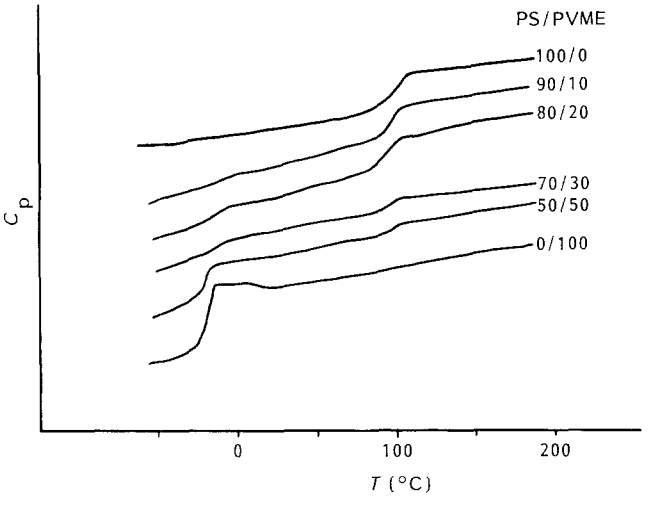


**Figure 2** D.s.c. traces of films of iPS and iPS/PVME blends after pre-melting at $T_c=270°C$

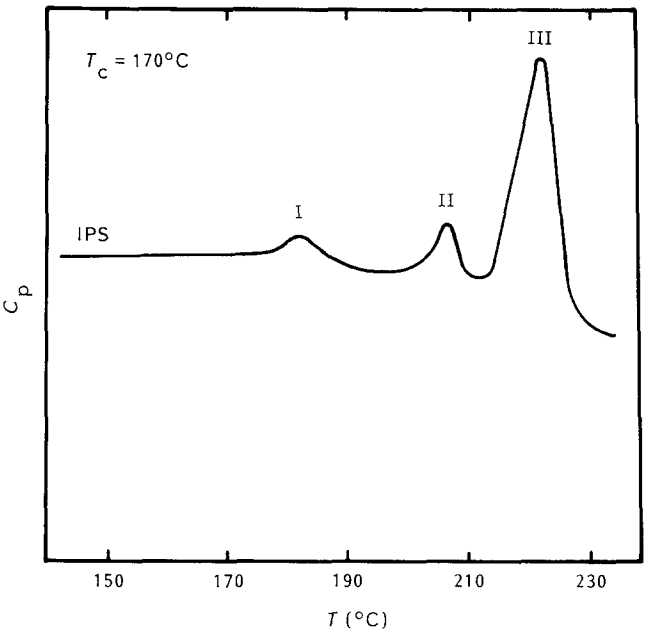


**Figure 3** D.s.c. thermograms of an iPS film crystallized isothermally at $T_c=170°C$

the pure iPS (97°C) whereas the $T_g$ of the PVME-rich phase (−22°C) is higher than that of the pure PVME (−27°C). The composition of these two phases depends on the phase diagram of the system and could be approximately found applying the Fox equation[11]:

$$\frac{1}{T_g(\text{blend})}=\frac{w(\text{iPS})}{T_g(\text{iPS})}+\frac{w(\text{PVME})}{T_g(\text{PVME})} \quad (1)$$

In this way the compositions of the two phases result to be 97/03 iPS/PVME for the iPS-rich phase and 06/94 iPS/PVME for the PVME-rich phase, respectively.

It should be noted that the intermediate $T_g$ present in the thermograms of the samples obtained by casting is not detected any more. This behaviour clearly indicates that phase separation of the homogeneous iPS/PVME mixture (intermediate phase) also occurs following the melting of the material obtained by casting.

*Melting behaviour*

*Figure 3* reports the d.s.c. thermograms of plain iPS. For all crystallization temperatures three peaks are always observed. As reported in the literature[9,12], the peak at the lowest temperature (peak I) corresponds to the melting of the material crystallized by secondary crystallization, and the peak at the highest temperature (peak III) is related to the melting of crystallites formed at $T_c$ but reorganized during the heating. Peak II, finally, is due to the melting of crystals formed at $T_c$ by primary crystallization.

The equilibrium melting temperature $T_m$ was obtained by using the Hoffman–Weeks equation[13]:

$$T_m'=T_m(1-1/\gamma)+T_c/\gamma \quad (2)$$

In Equation (2) $\gamma$ is the ratio of the real lamellar thickness to the thickness of the critical size nucleus and $T_m'$ is the observed melting temperature of the crystallites formed at $T_c$ (peak II). The equilibrium melting temperature $T_m$ resulted to be $230\pm2°C$.

The presence of PVME does not influence the melting behaviour of iPS. Three endothermic peaks are also

observed for the blends, whose position and ratio depend only on $T_c$, in contrast to what happened for two other blends containing isotactic polystyrene. In fact, in the case of iPS/PPO (poly(phenylene oxide))[12] a decrease in $T_m$ and $T_m'$ was observed with composition; such a decrease was attributed to the diluent effect of the non-crystallizable material. In the case of iPS/P(*o*CS-*co*-*p*CS) blends, which are phase-separated at $T_c$ (ref. 9), the presence of the copolymer modifies the ratio between the areas of the peaks.

The constancy of $T_m$ is probably due to the fact that the iPS/PVME blends are phase-separated (as reported previously) and the percentage of PVME in the iPS-rich phase is so small as to be not sufficient to influence in a detectable manner the melting temperature of iPS.

*Spherulite growth rate*

The values of the growth rate $G$ of iPS spherulites grown from iPS/PVME melt blends together with that of undiluted iPS are plotted in *Figure 4*. From *Figure 4* it can be seen that for iPS and for all blends $G$ shows a maximum for a $T_c$ ranging between 170 and 180°C, in agreement with the results reported in the literature by several researchers for pure iPS[9,14].

For a given $T_c$ the addition of PVME to iPS causes an increase of the crystallization rate. The size of this effect increases with the increase of PVME in the blends and may be explained, in agreement with the conclusion of ref. 1, by the increase of the mobility of the crystallizable chain in the melt, due to the presence of PVME. In fact, the viscosity of the material surrounding the crystallites decreases with the increases of PVME content, enhancing the rate of diffusion of the crystallizable chains to the growing crystals and hence the rate of crystallization.

In order to analyse the experimental growth rate data the equation of the kinetic theory of crystallization refined by Hoffman was used[15,16]:

$$G = G_0 \exp\{-U^*/[R(T_c - T_\infty)]\} \exp[-K_g/(\Delta T) T_c f] \quad (3)$$

In equation (3) $U^*$ is the activation energy for the transport of the crystallizable segments from the melt to the site of crystallization; $T_\infty$ is the temperature where any motion ceases, and can be related to $T_g$ ($T_\infty = T_g - C$, where $C$ is a constant). The term $K_g$ may take three different values depending on the way in which the secondary surface nuclei are formed and spread out on the existing crystal face:

$$K_g(\mathrm{I}) = 4 b_0 \sigma \sigma_e T_m / [(\Delta H_f) k] = K_g(\mathrm{III}) \quad (4)$$

$$K_g(\mathrm{II}) = 2 b_0 \sigma \sigma_e T_m / [(\Delta H_f) k] \quad (5)$$

Here $\sigma$ and $\sigma_e$ are the lateral and fold surface free energy, respectively, $b_0$ is the thickness of a monomolecular layer, $k$ is the Boltzmann constant, and $\Delta H_f$ is the melting enthalpy.

When the formation of a secondary surface nucleus is followed by rapid completion of the substrate, $K_g = K_g(\mathrm{I})$ (regime I of growth). If surface nuclei form in a large number on the substrate and spread out slowly, $K_g = K_g(\mathrm{II})$ (regime II of growth). When surface nuclei form in such a large number that the distance between two adjacent nuclei approximates the width of a stem, then $K_g = K_g(\mathrm{III})$ (regime III of growth).

Plots of $\alpha = \ln G + U^*/[R(T_c - T)]$ against $1/T_c(\Delta T)f$ should yield a straight line with $-K_g$ as slope. For pure iPS the data cannot be linearized with one or more straight lines with any selection of constants (see *Figure 5*), but the plot displays a curvature and consequently it is impossible to observe the regime transition regions. On the other hand, the iPS crystallizes in a very extended range of temperatures and should present the three-region behaviour according to the Hoffman theory. The deviation observed could be associated with the high molecular-weight dispersity of the samples that present, at a fixed $T_c$, mixed regime behaviour (re-examination of the growth rates of the iPS using monodisperse fractions might be fruitful in order to analyse the regime behaviour).

Growth rate data for the iPS crystallized from the blends were analysed as above to test their regime behaviour using equation (3). In theory we should have

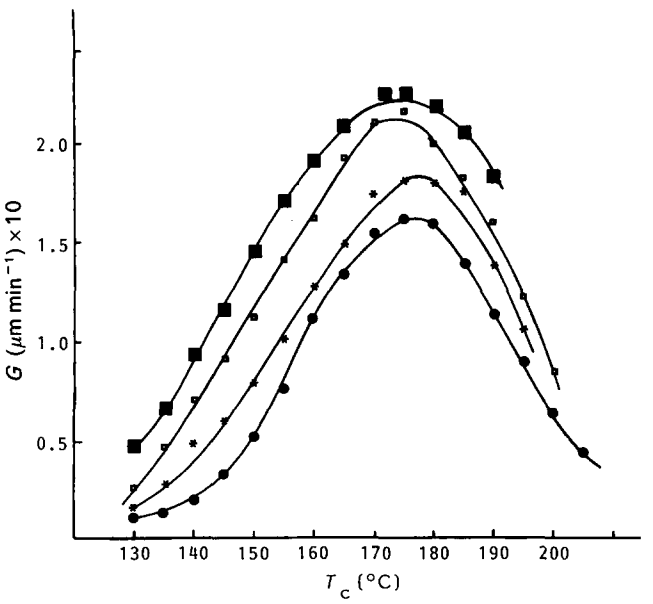


**Figure 4** Spherulite radial growth rate as a function of crystallization temperature for iPS and iPS/PVME blends: (●) iPS; (*) iPS/PVME 90/10; (□) iPS/PVME 70/30; (■) iPS/PVME 50/50

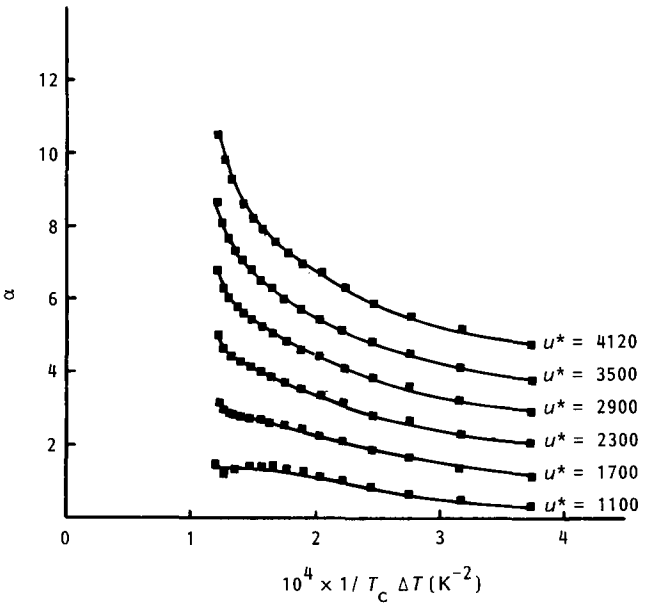


**Figure 5** Plots of $\alpha$ *versus* $1/(T_c \Delta T)$ according to equation (3) for the pure iPS for different values of $U^*$, setting $C = 51.6$

used the equation valid for blends, but this equation written as

$$\ln G - \ln \phi_2 \rightarrow \frac{U^*}{R(T_c - T_\infty)} - \frac{0.2 T_m \ln \phi_2}{\Delta T} = \ln G_0 \quad (6)$$

requires for its application the values of $T_g$, $T_m$ and composition $\phi_2$ of the iPS-rich phase. It should be noted, moreover, that in equation (6) the $U^*$ term contains the contribution of diffusional processes of the amorphous and crystallizable material to the growth rate. The facts that $\phi_2$ of the iPS-rich phase as estimated by the Fox equation seems to be close to 1 and that $T_m$ is constant with composition (at least as measured by the d.s.c. technique) justify the use of equation (1) also for the blends. There exist values of $U^*$ and $T_\infty$ that permit optimal linearization of the data (see *Figure 6* for example), which according to the theory could indicate a transition regime in the crystallization behaviour (regime III at low $T_c$ and regime II at higher $T_c$). Unfortunately the ratio of the slopes of the two lines is always higher ($\simeq 4$) than that predicted by the kinetic theory ($=2$) for all the selected values of $T_\infty$ and $U^*$. This, in disagreement with the kinetic theory of crystallization, could indicate that $\sigma$ and $\sigma_e$ in equation (1) are not constant with the crystallization regimes and that they change by passing from regime III to regime II.

In the application of equation (3) one should note the drawback present in any method that needs a multi-fitting procedure. A good fit of the parameters (in our case $C$ and $U^*$) does not necessarily ensure the physical reality of the system.

*Bulk crystallization*

The half-time of crystallization $\tau_{0.5}$ obtained from the isotherm of crystallization is plotted as a function of the crystallization temperature for the pure iPS and for the iPS/PVME blends in *Figure 7*. Two features are worth noting in these plots:

(1) The maximum of the overall crystallization rate is located between 170 and 180°C for all blend compositions, in analogy with the behaviour of the spherulite radial growth rate.

(2) For a given $T_c$, $\tau_{0.5}$ and hence the overall crystallization rate seem to be almost independent of the composition.

Thus, taking into account that overall bulk crystallization comprises the nucleation rate plus the spherulitic crystallization rate $G$, and that $G$ increases with the composition as discussed in the previous section, one can conclude that the nucleation process must be influenced negatively by the addition of PVME, in agreement with the morphological evidence (see next section).

The Avrami equation[17] was used to analyse the data of the bulk kinetics of crystallization

$$\ln[-\ln(1 - X_t)] = \ln K_n + n \log t$$

where $X_t$ is the weight fraction of crystallinity at time $t$, $n$ is the Avrami index and $K_n$ is the overall kinetic rate constant. The experimental data fit the Avrami equation well also at very long crystallization times, indicating that no observable secondary crystallization is present. The value of the Avrami index, contrary to the theoretical prediction, is non-integral and ranges between 2 and 3. These non-integral values are generally accounted for by mixed nucleation and crystallization modes. The Avrami index can suggest that, supposing that the nucleation mechanism is heterogeneous as discussed by Boon *et al.*[18] and taking into account that the morphology of the crystallized samples is spherulitic, two growth mechanisms can be present: two-dimensional at the beginning of the process and three-dimensional during further growth.

In the literature several examples, regarding the occurrence of both lamella and spherulites in bulk crystallization of polymers, have been reported[19–21]. In particular, recently Bassett and Vaughan[21] have shown that spherulites of iPS, crystallized from the melt, can have two-dimensional lamellar-shape-like precursors. This observation provides confirmation of our hypothesis.

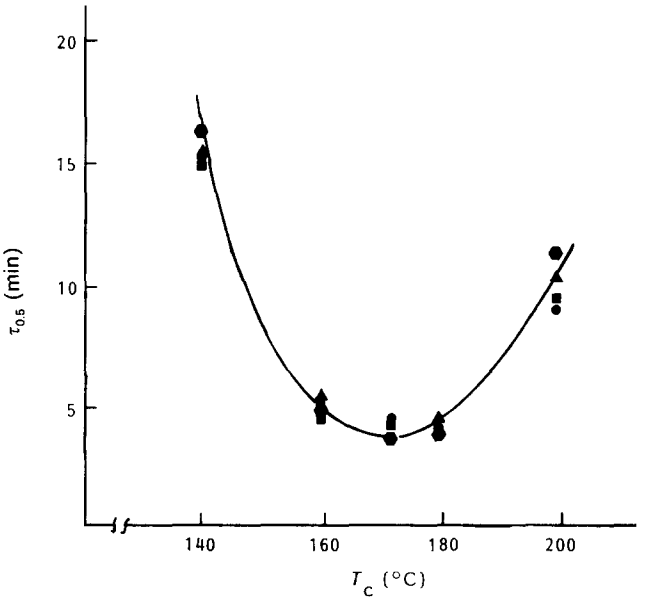


**Figure 7** Half-time of crystallization, $\tau_{0.5}$, as a function of crystallization temperature, $T_c$, for samples of different composition: (●) pure iPS; (▲) iPS/PVME 90/10; (●) iPS/PVME 80/20; (■) iPS/PVME 70/30

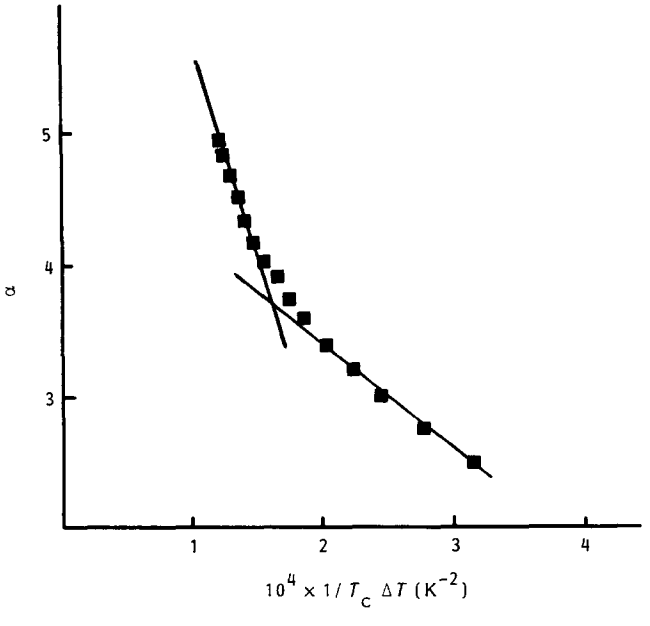


**Figure 6** Plots of $\alpha$ *versus* $1/(T_c \Delta T)$ according to equation (3), setting $C = 51.6$ and $U^* = 2500$

*Morphology and superstructure*

The morphology of the blends in the melt phase at 270°C is shown in *Figure 8*. For all blend compositions, small spherical domains dispersed in a melt matrix are present. In agreement with the $T_g$ results the matrix should be the iPS-rich phase and the dispersed spherical domains the PVME-rich phase. During crystallization, the iPS spherulites occluded droplet particles of PVME-rich phase in their intraspherulite region (see *Figure 9*).

The long spacing $L$ as measured on plain iPS and iPS/PVME blends is $155 \pm 10$ Å irrespective of crystallization temperature and blend composition. Therefore, the presence of PVME has no effect on the super-reticular distances, indicating that the PVME present in the iPS-rich phase can segregate during iPS crystallization essentially into interfibrillar regions of iPS. This result is also found in other crystallizable blends, for example iPS/aPS and PEO/iPMMA, where the amorphous material is rejected during crystallization into interfibrillar regions of crystallizable component spherulites.

The addition of PVME influences the apparent nucleation density of the semicrystalline iPS. In fact the dimensions of the iPS spherulites measured at the end of the crystallization process increase on increasing the overall PVME content in the blend (see *Figure 10*).

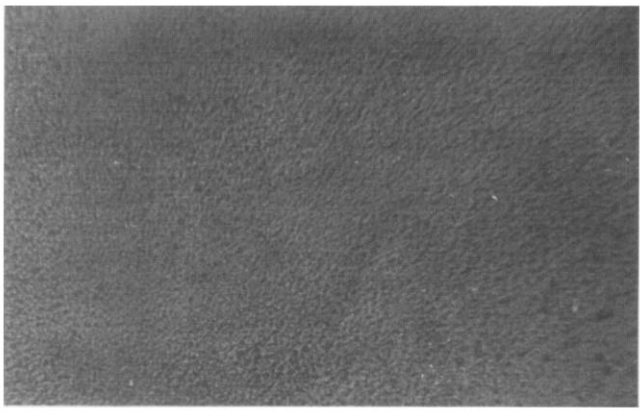

**Figure 8** Optical micrograph of a melt sample of iPS/PVME 90/10 blend (200×)

**Figure 9** Scanning electron micrograph of a fracture surface of iPS/PVME 90/10 blend, crystallized at $T_c = 180$°C (400×)

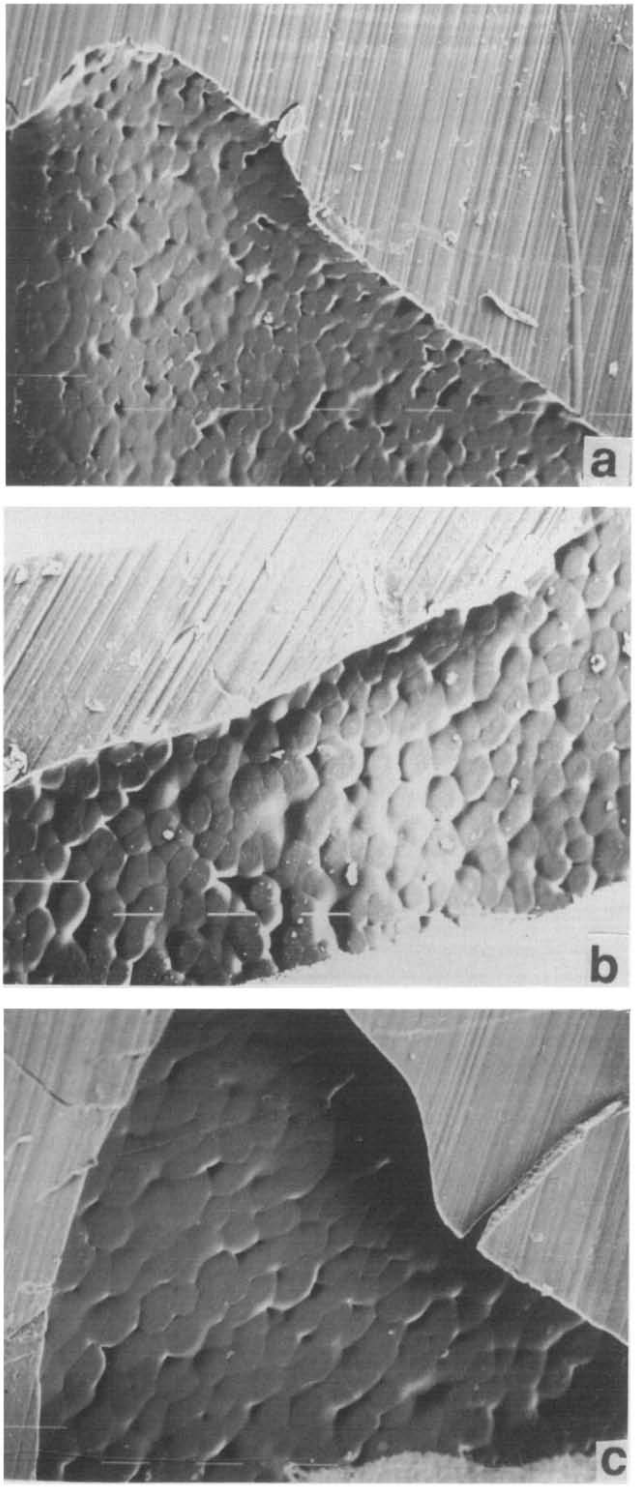


**Figure 10** Scanning electron micrographs of surfaces of samples crystallized isothermally at $T_c = 180$°C: (a) pure iPS; (b) iPS/PVME 90/10; (c) iPS/PVME 70/30 (60×)

At this point it is interesting to obtain the nucleation density from the overall crystallization rate constant $K_n$ and the spherulite growth rate $G$. In fact, assuming that the nucleation of iPS is heterogeneous (as reported in the literature[18]) and that the morphology is spherulitic, according to the kinetic theory of crystallization[22], we have the following relation:

$$K_n = \frac{4}{3}\pi N G^3 \frac{\rho_c}{\rho_a} \frac{1}{(1-\Lambda_\infty)} \tag{7}$$

**Table 3** Number of nuclei in 10 $\mu m^3$ of iPS/PVME (wt/wt) blend as a function of $T_c$ and composition

| | Composition, iPS/PVME | | |
|---|---|---|---|
| $T_c$ (°C) | 100/0 | 90/10 | 80/20 |
| 140 | 420 | 25 | 5.0 |
| 160 | 6.0 | 4.0 | 1.7 |
| 180 | 2.5 | 1.7 | 1.2 |
| 200 | 17 | 6.5 | 5.2 |

where $N$ is the nucleation density, $\rho_c$ and $\rho_a$ are the densities of the crystalline and amorphous phases, $\Lambda_\infty$ is the crystallinity at infinite time, $K_n$ is the overall growth rate constant obtained by using the relation[22] $\ln 2/(\tau_{0.5})^n$ and $G$ is the spherulite growth rate.

The values of $N$ are reported in *Table 3*. It can be seen that for a given $T_c$ in the case of blends $N$ is always lower than that of pure iPS, in agreement with the microscopic observation. This indicates that the PVME seems to reduce the nucleation ability of the iPS. This effect can be accounted for by assuming that some of the heterogeneous iPS nuclei can be dissolved in the PVME-rich phase during the mixing and pre-melting processes.

It is interesting to note that for $T_c = 200$°C the number of nuclei is higher than that for the sample crystallized at $T_c = 180$°C. This can be explained by assuming that the iPS heterogeneous nucleation process is not instantaneous. Therefore, because the growth rate at 200°C is strongly depressed with respect to that at $T_c = 180$°C (see *Figure 4*), at 200°C there is a larger uncrystallized volume in which the nuclei can develop, giving rise to an increase of the nucleation density.

## ACKNOWLEDGEMENT

This work was partially supported by 'Progetto Finalizzato del CNR: Chimica Fine II'.

## REFERENCES

1 Martuscelli, E., Sellitti, C. and Silvestre, C. *Makromol. Chem., Rapid Commun.* 1985, **6**, 125
2 Bank, M., Leffingwell, J. and Thies, C. *Macromolecules* 1971, **4**, 43
3 Bank, M., Leffingwell, J. and Thies, C. *J. Polym. Sci., Polym. Phys. Edn.* 1972, **10**, 1097
4 Kwei, T. K., Nishi, T. and Roberts, R. F. *Macromolecules* 1974, **7**, 667
5 Yang, H. E. Ph.D. Dissertation, University of Massachusetts, Amherst, 1985
6 Lu, F. J., Benedetti, E. and Hsu, S. L. *Macromolecules* 1983, **16**, 1525
7 Garcia, D. *J. Polym. Sci., Polym. Phys. Edn.* 1984, **22**, 107
8 Murray, C. T. Ph.D. Dissertation, University of Massachussets, Amherst, 1985
9 Silvestre, C., Cimmino, S., Karasz, F. E. and MacKnight, W. J. *J. Polym. Sci., Polym. Phys. Edn.* 1987, **25**, 2531
10 Silvestre, C., Cimmino, S., Martuscelli, E., Karasz, F. E. and MacKnight, W. J. *Polymer* 1987, **28**, 1190
11 Fox, T. G. *Bull. Am. Phys. Soc.* 1956, **2**, 123
12 Plans, J., MacKnight, W. J. and Karasz, F. E. *Macromolecules* 1984, **17**, 810
13 Hoffman, J. D. and Weeks, J. J. *J. Chem. Phys.* 1965, **42**, 4301
14 Boon, J. and Azcue, J. M. *J. Polym. Sci., Polym. Phys. Edn.* 1968, **6**, 885
15 Lauritzen, J. I. Jr and Hoffman, J. D. *J. Appl. Phys.* 1973, **44**, 4340
16 Hoffman, J. D. *Polymer* 1982, **24**, 3
17 Avrami, M. J. *J. Chem. Phys.* 1939, **7**, 1103
18 Boon, J., Challa, G. and Von Krevelen, D. W. *J. Polym. Sci. (A-2)* 1968, **6**, 1835
19 Keith, H. D. *J. Polym. Sci. (A)* 1964, **2**, 4339
20 Kovacs, A. J. in 'Structure of Crystalline Polymers' (Ed. I. H. Hall), Elsevier Applied Science, London, 1984
21 Bassett, D. C. and Vaughan, A. S. *Polymer* 1985, **26**, 717
22 Mandelkern, L. 'Crystallization of Polymers', McGraw-Hill, New York, 1964